Electromagnetic Waves), Sovetskoe radio, M., 1970, p. 462.
[17]V. B. Gil'denburg and S. V. Golubev, Zh. Eksp. Teor. Fiz. 67, 89 (1974) [Sov. Phys. JETP 40, 46 (1974)].
[18]G. A. Askar'yan, Zh. Eksp. Teor. Fiz. 42, 1567 (1962) [Sov. Phys. JETP 15, 1088 (1962)].
[19]A. G. Litvak, V. A. Mironov, G. M. Fraiman, and A. D. Yunakovskii, Fiz. Plazmy 1, 60 (1975) [Sov. J. Plasma Phys. 1, 31 (1975)].

Translated by J. G. Adashko

Thermodynamic properties of a nonideal argon or xenon plasma

V. K. Gryaznov, M. V. Zhernokletov, V. N. Zubarev, I. L. Iosilevskiĭ, and V. E. Tortov

Division of the Institute of Chemical Physics of the USSR Academy of Sciences
(Submitted 21 June 1979)
Zh. Eksp. Teor. Fiz. 78, 573–585 (February 1980)

Results are presented on shock-wave dynamic compression and on the investigation of the equation of state of a strongly nonideal argon and xenon plasma. The experiments were performed with explosive propelling devices, using the energy of the detonation of powerful condensed explosives. A considerable increase of the pressure and a decrease of the internal energy are established. This is a consequence of the deformation of the electronic energy levels of the strongly compressed plasma. A quantum-mechanical model of a bounded atom and a pseudopotential model of a plasma are proposed to describe this effect.

PACS numbers: 52.25.Kn

1. INTRODUCTION

The operation of many contemporary technical devices is based on concentration of appreciable energy in dense media,[1-3] which leads to the production of a high-pressure plasma with strong interparticle interaction. The theoretical description of the physical processes in a nonideal plasma entails considerable difficulties of correctly accounting for the varied and structurally complicated multiparticle interactions, and is possible at the present time only in the limit of low density by the methods of perturbation theory,[4,5] or in the case of idealized systems by computer-experiment methods.[6,7] The main source of information on the properties of strongly compressed plasma in this situation is experiment, which makes it possible to establish the limits of applicability of the asymptotic approximation and which yields the required information for the construction of thermodynamic models of a strongly nonideal plasma.

Experiments with a nonideal plasma call for high local concentrations of the energy in dense media and for the use of diagnostics methods that are not traditional in plasma physics. This is due to the patently insufficient number of thermodynamic measurements made in the region of advanced nonideality.[8-13] In particular, there are no systematic investigations of the region of extremely high plasma densities, where strong interparticle interaction manifests itself not only in the continuous spectrum, but also causes distortion of the discrete energy levels of the electrons bound in the atoms and ions.[1,7]

In this paper we present the result of investigations of the thermodynamic properties of a dense nonideal plasma of argon and xenon, obtained by compression and by irreversible heating of the gases in the front of high-power ionizing shock waves produced when powerful condensed explosives are detonated. The combination of electronic-contact and optical basic methods has made it possible to register the kinematic characteristics of the motion of the shock waves and, by using the mass, momentum, and energy conservation laws to obtain the equations of state of a dense shock-compressed plasma.

The experiments yielded shock waves with velocities up to 9.6×10^5 cm/sec. The plasma generated thereby has a high temperature $T\sim(2-6)\times10^4$ K and a pressure $P\sim1-6$ kbar, and its density approaches that of the liquid phase (see Figs. 4a and 4b below). Thus, the plasma investigated in the experiment is nonideal with respect to a broad spectrum of interparticle interactions with substantial participation of excited states of atoms and ions.

2. EXPERIMENTAL TECHNIQUE

Experiments on shock compression of inert gases were performed with generators of rectangular shock waves using explosive driving systems.[14,12,15] In these devices, the metallic flyer plates were accelerated to 5–6 km/sec by the detonator products of charges of powerful condensed explosives. The high uniformity and reproducibility of the dynamic parameters of the generators was attained by using specially shaped detonation lenses, flyer plates of special construction, as well as by using active charges with geometrical dimensions sufficient to establish stationary detonation. The collision of the moving flyer plates with the condensed targets produces in the latter shock waves with maximum pressures of the order of 1 Mbar. The emergence of the wave to the interface between the target and high-pressure inert gas is accompanied by expansion of the target material in the centered release wave

 0038-5646/80/020288-08$02.40

and by formation of a secondary shock wave, which compresses, accelerates, and ionizes the investigated gas.

The characteristics of the shock-compressed plasma were changed by using active explosive charges with various geometrical dimensions, and also by varying the thicknesses and materials of the flyer plates driven by the explosion. Most experiments were performed with explosion generators having the parameters listed in Table I. Special gasdynamic measurements have shown that the parameters of the employed generators have a reproducibility not worse than 1–2% at a curvature radius of the front of the driving shock wave in the target at a level of 0.5 m.

To increase further the velocity and the pressure of the generated shock waves in the plasma, the effect of evaporation of the target material in an isentropic release wave was used.[16] In this case the targets were made of porous copper, and this increased the effects of viscous dissipation, and consequently the entropy of the shock compression, making it sufficient[16] for partial evaporation of the target material in the course of its adiabatic expansion. Thus, the use of a copper target with porosity $m = \rho_0/\rho_{00} = 3$ in place of a solid aluminum target made it possible to increase the shock wave velocity in argon ($P_0 = 1$ atm) from 7.77 to 9.44 km/sec.

In accordance with the dynamic approach,[14,17] to determine the equation of state of shock-compressed matter it is necessary to register independently two kinematic parameters that characterize the propagation of a stationary shock wave in the investigated matter. In the present study, in analogy with experiments on shock compression of condensed media, we measured the velocity D of the shock-wave front and the mass velocity u of the shock-compressed plasma. To measure the mass velocity u we used electric contacts screened by thin metallic foil that prevented operation of the pickup at the instant of arrival of the shock-wave front. The quality of operation of the screened electric contacts was verified in a special series of methodological experiments by varying the thickness and material of the foil, and also the gap between the foil and the contacts. We compared the operation of the screened and open electric contacts in helium and propane atmospheres in which, in view of the low degree of ionization, both systems of pickups were operated simultaneously at the instant of arrival of the heavy contact surface of the target. To monitor the stationary character of the flow and to take into account the possible skewing of the front of the shock wave, eight pairs of electric contacts, with different bases, were uniformly placed over two coaxial circles with different radii.

The shock-wave front velocity D was measured by an optical basis method, by registering the light emission from the front. The transition of the shock wave from the target into the investigated gas leads to the appearance of intense emission (zero—on Fig. 1a), which is recorded in the form of a light band with a streak camera. The encounter of the shock wave with a Plexiglas barrier located at a specified distance from the target leads (instant D, Fig. 1) to an increase of the intensity of the emission, and consequently determines the front velocity D. The arrival at the barrier of the intense shock wave reflected from the metallic piston destroys the barrier, a fact manifest by loss of its transparency and by cutoff of the radiation at the instant u that determines (jointly with the electric contacts) the mass velocity of the plasma. With increasing initial gas pressure, the amplitudes of the pressure of the incident shock waves increase, and this causes destruction of the Plexiglas barriers even at the instant of the first shock. This circumstance makes difficult reliable optical registration of the mass velocities of shock waves with maximum pressures exceeding ~20 kbar.

In addition, with increasing initial gas density and intensity of the shock waves, the streak photographs reveal more and more clearly a fine structure consisting of alternating light and dark bands (Fig. 1b). Special experiments in which the measurement base was varied have shown that the dimensions of the bands are proportional to the base, and replacement of Plexiglas by other transparent materials (lead glass, lithium fluoride, polystyrene, etc.) yields the same but less distinct general picture of the bands. It appears that the short-wave radiation emerging from the shock-wave front (equilibrium temperature up to 6×10^4 K, light flux ~10^8 W/cm^2) heats and evaporates[18] the thin (several microns) Plexiglas layer, which is opaque to short-wave radiation with $\lambda \lesssim 3000$ Å. The motion of this evaporated layer forms a weak shock wave whose interaction with the incident flux leads in fact to the fine structure of emission on Fig. 1b, recorded with the streak camera. An indirect confirmation of this picture is offered also by the decrease of the intensity of the registered emission as the shock wave propagates in the gas (Fig. 1b). In accordance with this flow scheme, the instant of arrival of the front of the incident wave at the internal surface of the window was taken to be the first flash of light D on Fig. 1b. As shown by detailed gasdynamic calculations, one can neglect the change in the back-wave velocity as the result of interaction with the plasma cushion of evaporated Plexiglas. We note that the correctness of this interpreta-

TABLE I. Parameters of explosive driving devices.

Number of experimental setup	Material and thickness of flyer plate, mm	Flight distance of flyer plate, mm	Velocity of flyer plate, 10^5 cm/sec	Material and thickness of screen of experimental assembly, mm	Material and thickness of target, mm	Parameters of shock wave in target	
						u, 10^5 cm/sec	P, kbar
1	Al (4,0)	40	5.44	Al (3)	Cu (1.5)	1.75	1023
2	Al (4,0)	40	5,44	Al (4)	Al (1.5)	2,72	664
3	Fe (2,20)	70	5.0	Fe (2.5)	Al (1.5)	3.30	875
4	Fe (1,10)	60	5.87	Fe (1,0)	Al (1.0)	3.87	1107

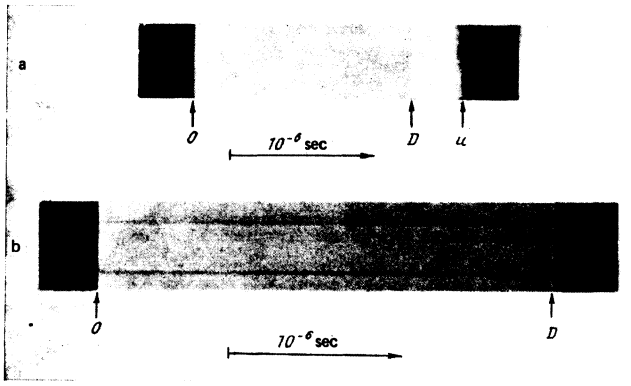

FIG. 1. Typical streak photograph of shock-wave process (thickness of the entrance slit of the instrument 0.1 mm): 0—emergence of the shock wave from the target to the gas, D—reflection of the shock wave from the transparent screen, u—impact of target against the screen. The arrow shows the scanning direction and indicates the time scale. a) Argon, P_0 = 1 atm, magnification 5×; b) xenon, P_0 = 10 atm, magnification 6×.

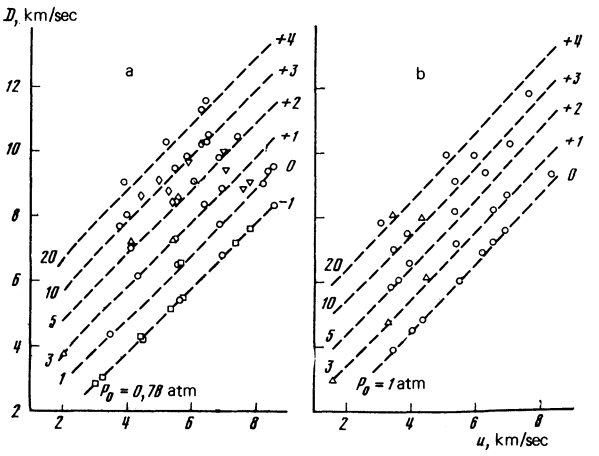

FIG. 2. Dynamic adiabats of argon (a) and xenon (b) (on the left of the curves are indicated the initial gas pressures P_0, and on the right the shift of each plot in the D direction in km/sec): ○—present paper, □—[10], ◇—[11], △—[12], ▽—[19], dashed—calculation.[20]

tion of the streak photographs is confirmed independently by the results of probe[12] and x-ray[11] measurements (see Figs. 2a and 2b).

The generation method used by us produces in the plasma pressures and temperatures greatly exceeding the thermal endurance of the construction materials used in the apparatus. In this case it becomes possible to realize inertial containment of the plasma for a short time determined by the spreading of the construction elements of the explosive experimental setups. It is precisely these circumstances which determine the geometrical dimensions and the lifetimes of the plasma with constant parameters in the dynamic experiments. To obtain one-dimensional and stationary flow of a shock-compressed plasma in the registration zone we performed, for each type of explosive driving setup, gasdynamic calculations of the motion of the shock waves and of the rarefaction waves propagating from the contact and from the free boundaries of the experimental installations. The influence of the lateral release waves was eliminated by preparing flyer plates and targets in the form of wide thin disks with relative diameter to thickness ratio ~30–40. The base of the dynamic measurements was determined by the arrival of the perturbations from the rear side of the flyer plate and ranged from 3 to 8 mm, depending on the actual conditions.

3. EXPERIMENTAL RESULTS

The obtained experimental data are shown in Fig. 2a, and some of them are shown in Tables II and III, which give, besides the measured values of D and u, also the values calculated in accordance with the conservation laws for the pressures P, the specific volume V, and the specific enthalpy H of the shock-compressed plasma. The same figure shows the plasma parameters calculated in accord with a number of thermodynamic models. Each experimental point in Table II or III is the result of the averaging of 3–5 experiments with eight independent probe measurements in each. The errors in the registrations of D(~1%) and of u(~1.5–2 %) lead to uncertainties ~7–19 % and ~3–5 % in the values of the volume V and enthalpy H, respectively. The experimental results, in terms of the kinematic variables are shown in Fig. 2 and are compared with results of measurements of shock adiabats by x-ray,[11] probe, and optical methods using metal and polymer targets,[10,11] as well as targets made up of condensed explosives.[19] It is seen that the different procedures of determining

TABLE II. Thermodynamic properties of shock-compressed argon.

Experiment						Theory						
						Ring approximation[20]					Model (2-5)	
P_0, atm	D, km/sec	u, km/sec	P, kbar	V, cm³/g	$H\cdot10^4$, J/g	V, cm³/g	$T\cdot10^{-3}$, K	$n_e\cdot10^{-18}$, cm⁻³	Γ	n_0*	V cm³/g	$T\cdot10^{-3}$, K
0.78	7.78	6.94	0.692	86.0	30,1	88,2	22,0	0,642	0,843	0,00422	90,6	21,6
1,0	6,5	5.59	0,597	87	20,9	81,7	19,5	0,401	0,798	0,0057	85,5	19,1
3,0	7.93	6,97	2,73	25,0	31,1	24,0	24,3	2.23	1.35	0.016	25,6	23,0
5,0	6,51	5.52	2.96	18,8	20,9	17.45	21,3	1,63	1,4	0,0277	19,9	19,9
10.0	7,8	6,52	8,19	8,78	28,4	7,8	25,1	5,405	2,01	0,055	9,06	22,3
20,0	7,35	6,28	15,4	4.47	26,6	4,05	25,3	8,68	2,51	0,113	5,19	20,5
20,0	7.65	6,4	16.2	5,01	28,6	4,00	26 0	9,77	2,54	0,11	5,0	21.3

TABLE III. Thermodynamic properties of shock-compressed xenon.

Experiment						Theory: Ring approximation[20]					Theory: Model (7-14)	
P_0, atm	D, km/sec	u, km/sec	P, kbar	V, cm^3/g	$H\cdot10^{-3}$, J/g	V, cm^3/g	$T\cdot10^{-3}$, K	$n_e\cdot10^{-20}$, cm^{-3}	Γ	$n\sigma^3$	V, cm^3/g	$T\cdot10^{-3}$, K
1.0	4.58	4.11	1.02	19.3	10.4	18.8	21.0	1.33	1.31	0.0163	21.0	21.6
3.0	7.81	7.00	8.99	6.43	30.2	6.00	42.0	9.71	1.38	0.051	7.07	41.7
5.0	6.35	5.39	9.49	5.56	19.7	3.77	33.1	11.4	1.99	0.0812	4.62	33.7
10.0	6.23	5.4	19.2	2.38	19.1	1.83	34.0	22.0	2.64	0.168	2.34	35.1
10.0	8.93	7.69	39.2	2.48	39.1	1.94	55.8	34.9	1.78	0.158	2.40	55.4
10.0	4.11	3.52	8.27	2.56	8.32	2.04	21.6	7.2	2.91	0.150	2.4	23.4

the equations of state of the high-pressure plasma are mutually consistent. In the investigated velocity range these data can be described by the relation $D=a+bu$, where in the case of argon $a=0.75, b=1.03$ at $P_0\sim1$–3 atm and $a=0.81, b=1.04$ at $P_0\sim5$–20 atm, while for xenon $a=0.10, b=1.10$ at $P_0\sim1$–3 atm and $a=0.10, b=1.14$ at $P_0\sim20$ atm.

The plasma states generated by the chosen driving unit and by the type of target correspond to a fixed release isentrope of the target material; this offers an additional possibility of monitoring the plasma parameters obtained from measurements and from the conservation laws, and also by verifying the compatibility of the experimental data at various pressure levels. To this end, the results of the measurements were plotted in the variables P and u, in view of the fact that the pressure and mass velocity are continuous on the contact surface separating the target from the gas.[21] An example is shown in Fig. 3, where the expansion isentropes were obtained by mirror reflection of the dynamic adiabats of solid aluminum in terms of the variables P and u.[14] We note that in this manner it is possible not only to verify the compatibility and the accuracy of the recorded dynamic parameters of the plasma, but also to monitor the satisfaction of the conservation laws in algebraic form on the shock-discontinuity front.

4. ANALYSIS OF THE EXPERIMENTAL RESULTS AND COMPARISON WITH THE THEORETICAL MODELS

At gas densities of the medium ($\rho \ll \rho_{cr}$) the most widely used at present is the quasichemical method of description (the "chemical model" in plasma theory[22]

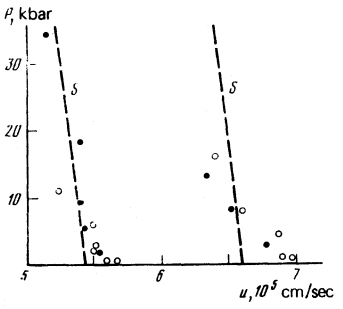

FIG. 3. P–u diagram of generation of plasma: ○—argon, ●—xenon, S—expansion isentropes of aluminum targets.

and the "mixture model" in the theory of neutral chemically reacting gases[23]), wherein the medium is regarded as an ideal mixture of particles of different sorts, the ratio between which is regulated by the equations of the chemical and ionization equilibrium, and the interparticle interaction is taken into account by the corresponding corrections that supplement the ideal-gas relations. At condensation densities ($\rho>\rho_{cr}$) one frequently uses a cell description, wherein the medium is broken up into atomic cells within which the charge distribution is calculated by the quasiclassical Thomas-Fermi model[24] or by using more accurate self-consistent quantum-mechanical approximations.[25]

Let us estimate the characteristic degrees of ionization of the plasma. The experimentally measured quantities yield direct information on the caloric equation of state $E=E(P, V)$. In this representation, the passage of each ionization corresponds to a transition region between the limiting relations $E=3/2PV$, $E=3/2PV+NJ_1$, $E=3/2PV+N(J_1+J_2)$ etc., where N is the number of nuclei and J_k are the ionization potentials. If we disregard the excitation of the internal degrees of freedom and the energy of the interparticle interaction, then the entire difference between the $E(P, V)$ dependence on the limiting function $3/2PV$ is determined by the energy lost to ionization. This leads to the following estimate of the experimentally attained degrees of plasma ionization: up to 0.7 for argon and up to 1.9 for xenon.

For more detailed estimates we use calculation results wherein the calculation of the internal partition functions of the atoms and ions take into account excited states with binding energies exceeding kT, while the corrections for the Coulomb interaction are described in the ring approximation in the grand canonical ensemble.[20] Using this approximation, we calculated the temperature, composition, and non-ideality parameters of the plasma from the experimental values of P, V, and $H=E+PV$; these are given in Tables II and III. It is seen that most experimental data pertain to the region where the charged subsystem is strongly nonideal:

$$\Gamma=e^2/kTr_D\geqslant1, \quad r_D=\left(kT/4\pi\sum Z_i^2e^2n_i\right)^{1/2} \qquad \text{(a)}$$

is the Debye radius, and the approximate calculation method used for the estimate describes only part of the experimental data. The difference has in this case a systematic character and increases with increasing plasma density in proportion to the increase of both the degree of Coulomb nonideality and to the nonideality due

to the interaction with participation of neutral atoms.

At the attained temperature level [$T \sim (20-60) \times 10^3$ K $\gg T_{cr}$], the van der Waals attraction is negligible and the primary role is assumed by repulsion at short distances, characterized by the parameter $n\sigma^3$ (Tables II, III), where the size of the atom or ion is assumed in accordance with Ref. 26 to be $\sigma_{Ar} = 3.405$ Å, $\sigma_{Xe} = \sigma_{Xe^+} = \sigma_{X^{++}} = \sigma_{Xe^{++}} = \sigma_{Xe^{+++}} = 4.055$ Å. The simplest estimate of the contribution of the short-range repulsion can be carried out[27] within the framework of the approximation of the second virial coefficient, calculated for a Lennard-Jones potential.[26] It is important that the characteristics of these potentials are constructed[28] on the basis of experimental data obtained at moderate temperatures, when the overwhelming majority of the atoms are in the energy ground states. The comparison of the results of these estimates with the experimental shock adiabats of Ar and Xe, shown in Fig. 4, indicates that the agreement improves noticably but at large compressions a systematic difference still remains and points to the presence of additional repulsion in the system. Indeed, at the high temperatures and pressures which are characteristic of the experiments, an appreciable fraction of the atoms and ions are in excited states, for which the short-range repulsion parameter exceeds the corresponding parameter for the atom in the energy ground state. This gives grounds for assuming that under our conditions the surrounding medium should cause deformation of the bound states and distort their contribution to the thermodynamic functions of the compressed plasma.

To describe this effect we must resort to a quantum-mechanical model that takes into account the action of the plasma environment on the ground and excited states of the atoms and ions in a dense plasma. Calculation for hydrogen within the framework of the simplest model[30,31] has shown that the influence of the deformation of the discrete spectrum comes into play at $\rho \gtrsim \rho_{cr}$. In the present paper, within the framework of the Hartree–Fock method, we calculated the influence of the compression on the energy spectrum and on the wave functions of multielectron atoms and ions. We consider a phenomenological model in which the influence of the surrounding medium on the intra-atomic and interatomic electrons is approximately taken into account by introducing the effective potential

$$\Phi(r) = \begin{cases} -Ze^2/r, & r < r_c \\ \infty, & r \geqslant r_c \end{cases} \quad (1)$$

The eigenfunctions and excitation energies of the atoms and ions in the potential (1) are calculated with the aid of one of the variants of the Hartree-Fock method, where the wave function of the atom is sought in the form of a linear combination of determinants made up of single-electron wave functions:

$$\psi_{nlms}(r, \theta, \varphi) = r^{-1} f_{nl}(r) Y_l^m(\theta, \varphi) \chi(s).$$

The coefficients of this linear combination are determined from the condition that the total wave function of the atom be the eigenfunction for the operators of the total orbital and spin angular momenta of the system. The use of the variational principle of quantum mechan-

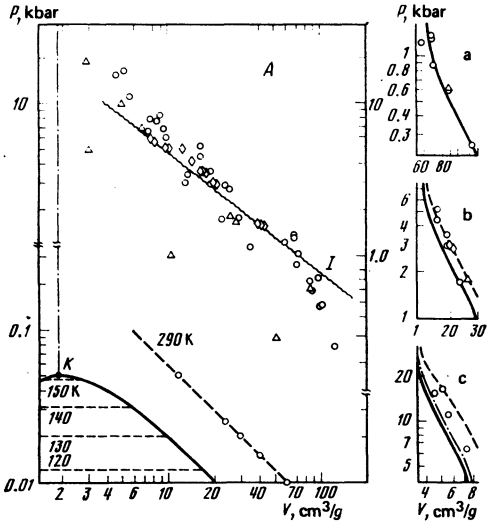

FIG. 4. A) Phase diagram of argon. The boundaries of the two-phase region are marked, the critical point is K; ○—present experiment, △—data of Ref. 12 corrected to account for the real equation of state of the gas[29] ahead of the shock-wave front, ◇—Ref. 11, dashed—isotherms,[29] dash-dot—the isochore $V = V_{cr}$, wavy line—boundary of single ionization $I(\chi_{Ar^+} = \chi_{Ar}, \chi_{Ar} = N_{Ar}/N_{tot})$. On the right is shown a comparison of the experimental shock adiabats with the results of model calculations. Solid curves—allowance for the interaction of the charged particles in the ring approximation, dash-dot—additional allowance for the interaction of the atoms in the approximation of the second virial coefficient,[26] dashed lines—calculation using the model of the "bounded atom": a) $P_0 = 1$ atm; b) $P_0 = 5$ atm; c) $P_0 = 20$ atm.

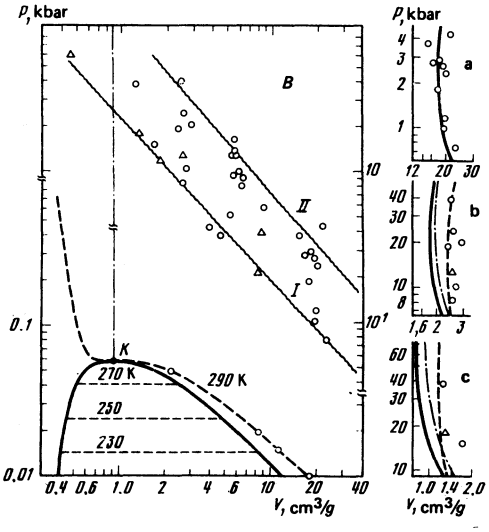

FIG. 4. B) Phase diagram of xenon. The notation is the same as in Fig. 4A. The boundary of the double ionization $II(\chi_{Xe^{++}} = \chi_{Xe^+})$ is shown in addition. On the right is shown a comparison of the experimental shock adiabats with the result of model calculations. Solid curves—calculation using the ring approximation; dash-dot—additional allowance for the interparticle repulsion in the approximation of the second virial coefficient.[26] Dashed lines—allowance for the interaction of the charged particles in the model (7–14) (the depth of the pseudopotential (6) and the boundary of the intra-atomic states are assumed equal to $-kT$): a) $P_0 = 1$ atm; b) $P_0 = 10$ atm; c) $P_0 = 20$ atm.

ics leads to the system of equations[32]

$$\left[\frac{d^2}{dr^2}+2V_{nl}(r)-\frac{l(l+1)}{r^2}-\varepsilon_{nl}\right]f_{nl}(r)$$
$$=\int_0^{r_c}G_{nl}(r,r')f_{nl}(r')dr'+\sum_{n'\neq n}\varepsilon_{nl,n'l}f_{n'l}(r), \quad (2)$$

where $V_{nl}(r)$ is a self-consistent potential that includes the interaction of the electrons with the nucleus and with one another. The integral in the right-hand side of (2) is the nonlocal part of the potential, or the exchange term, and is calculated (in the total-exchange approximation) without any additional simplifications, while $\varepsilon_{nl,n'l}$ and ε_{nl} are off-diagonal factors and the eigenvalues determined from the conditions

$$f_{nl}(0)=0, \quad f_{nl}(r_c)=0, \quad (3)$$

$$\int_0^{r_c}f_{nl}(r)f_{n'l}(r)dr=\delta_{nn'}. \quad (4)$$

The secondary boundary condition on (3) corresponds to the potential (1).

Solving the system (2) for different r_c, we can obtain the dependence, on the parameter r_c, of the partition functions which will be used subsequently to calculate the composition and the thermodynamic functions of the plasma. The equilibrium value of r_c corresponding to specified V and T are determined from the condition of the minimum of the free energy:

$$\left(\frac{\partial F}{\partial r_c}\right)_{V,T}=0, \quad (5)$$

where

$$F=kT\left\{N_e\ln\frac{n_e\lambda_e^3}{2e}+\sum N_k\ln\frac{n_k\lambda_k^3}{eZ_k(r_c)}\right\}+\Delta F_{\text{Coul}}+\Delta F_s$$

depends on r_c via the partition functions of the atoms and ions Z_k, and also via the approximate correction ΔF_s for the hard-sphere interaction.[33]

In contrast to the cell models of solids,[25] our approximation is constructed within the framework of the quasi-chemical method of description with explicit allowance for the translational degrees of freedom of the individual species of particles. The electrons are divided into two species and are located both inside and outside the cells, while the volume occupied by the atomic or ionic cell $4/3\pi r_c^3$ constitutes only part of the average volume per nucleus. In the calculation of the partition function in Ref. 34, the particle is assigned the average volume per particle, whereas in the calculation of the hard-sphere repulsion a much smaller volume is assigned, starting with which the ground state shifts noticably. In papers devoted to the theory of the condensed state[35] a cell radius r_c is semi-empirically chosen such that the calculated first maximum of the radial distribution function of the hard-sphere system coincides with the experimentally measured value for a given density. Using a thermodynamically consistent procedure of choosing $r_c(V,T)$ and the standard technique of calculating the thermodynamic equilibrium,[20] we calculated the shock adiabats of argon (Fig. 4). It is seen from the comparison that the obtained shift of the Hugoniot adiabats reflects correctly the tendency revealed in experiments with Ar and Xe, but exceeds the necessary value, especially at densities close to critical. The apparent reason is that the hard-sphere approximation assumed in the model described above greatly overestimates the real repulsion between the atoms at close distances, for a quantitative description of which the model of "soft" spheres[36] is more adequate.

A feature of the quasichemical description under conditions of a strongly nonideal plasma is the arbitrariness of separation of the charges into free and bound ones. As a result, the effect considered by us as a distortion of the contribution of the excited states can be treated in the case of a different separation into species as a manifestation of the quantum character of the electron-ion interaction at close distances. Approximate allowance for this effect in the chemical model of the plasma is made by introducing the effective paired electron-ion pseudopotential,[22,37] which differs from the Coulomb potential at short distances. As a result, under conditions of strong compression, the corresponding corrections for the interaction of the free charges are no longer functions of only the Coulomb nonideality parameter Γ, but are determined by the concrete electronic structure of the given chemical element and by the choice of the position of the boundary that separates the free and bound states. Under condition of weak nonideality the form and parameters of the pseudopotential can be calculated from the known wave functions of the isolated atom.

Under conditions of strong nonideality the form of this potential is indeterminate. Nonetheless, the successful experience in constructing extrapolation approximations in the single-component model of the plasma[38] gives grounds for hoping to reduce the problem to a semi-empirical choice of the parameters of a successfully selected pseudopotential, and of obtaining a satisfactory thermodynamic description of a dense plasma. We use the binary pseudopotential proposed in Ref. 39, which is close in form to that calculated for hydrogen in a number of papers[22,37]

$$\Phi_{ie}=-\frac{Z_ie^2}{r}(1-e^{-r/\varkappa}), \quad \Phi_{ei}=\frac{e^2}{r}, \quad \Phi_{ij}=\frac{Z_iZ_je^2}{r}, \quad (6)$$

and $\varkappa$ is a free parameter. Following Ref. 38, we choose the binary correlation function in the form

$$F_{\alpha\beta}(r)=1\pm A\frac{e^{-qr}-e^{pr}}{r}\equiv 1\pm\Psi_0e^{-\nu r}\frac{\operatorname{sh}\omega r}{\omega r}. \quad (7)$$

The general functional form of (7) is obtained[39] within the framework of the ring approximation for the potential (6), which is valid in the limit $\Gamma\ll 1$, while the parameters A,p,q (or Ψ_0,ν,ω), which enter in (7), are determined from the conditions of screening[38,40] and of the approximate connection between the amplitude of the screening cloud Ψ_0 with the pseudopotential depth $\Phi_{ei}^*(0)$:

$$n\int[F_+(r)-F_-(r)]d\mathbf{r}=1, \quad (8)$$

$$n\int[F_+(r)-F_-(r)]\frac{r^2}{r_D^2}d\mathbf{r}=3, \quad (9)$$

$$-\Psi_0\approx-\ln F_+\approx\beta[\Phi_{ei}^*(0)-\Delta\mu_e-\Delta\mu_i]. \quad (10)$$

The corrections to the thermodynamic quantities, expressed in terms of the correlation functions, are given

by

$$U=-Vn\int\Phi_{xyz}(F_+-F_-)\,d\mathbf{r}, \tag{11}$$

$$\Delta E=Vn^2\int[F_+\Phi_{ei}^*+F_-\Phi_{ii}^*]\,d\mathbf{r}, \tag{12}$$

$$\Delta PV=\tfrac{1}{3}(2\Delta E-U), \tag{13}$$

$$\Delta\mu_i=\Delta\mu_e\approx(2N)^{-1}\Delta E, \tag{14}$$

where U is the potential energy of the interaction and μ_i and μ_e are the chemical potentials of the free charges. The relation (12) is then exact when the pseudopotential (6) does not depend on the thermodynamic parameters, while (13) is a consequence of the virial theorem.[26]

The basic free parameter $\Phi_{ei}^*(0)$ of the model—the depth of the pseudopotential—is chosen to fit the experimental data, the results of the dynamic compression of cesium by shock waves.[8,9] A comparison of the results obtained with different $\Phi_{ei}^*(0)$ shows[41] that the best description of the experiment[8,9] is obtained in the case when the depth of the potential is equal to the energy that separates the free particles from the bound ones. A comparison of this model with the results of shock compression of inert gases (Fig. 4b) shows that this model provides an acceptable description also of this experimental information. Thus, two independent groups of experimental data indicate already that within the framework of the aforementioned model the effective depth of the pseudopotential should be much lower than the value recommended in Ref. 37 and calculated using the wave functions of the isolated hydrogen atom.

It follows from the foregoing comparison that even at the degrees of compression attainable in the given dynamic experiment the thermodynamic properties of a dense strongly nonideal Ar or Xe plasma can be satisfactorily described within the framework of the quasichemical model using the above-described theoretical model. In the more rigorous plasma-theory approach, called arbitrarily the "physical" model of the plasma[22] (its analog is the "model of initial atoms" in the theory of neutral gases[23]), the zeroth approximation employed is a system of noninteracting nuclei and electrons. In this approach, both the interaction in the continuous spectrum and the formation of bound complexes are considered jointly within the framework of a single expansion of the thermodynamic potential in powers of the activity.[42] In practice, the calculation of the terms of this expansion is very difficult and is limited in fact to the pair approximation, and consequently, without loss of rigor, the results of this approach are valid only for a hydrogen plasma.[43] Nonetheless, the approximate relations obtained in Ref. 42 are frequently employed also within the framework of the "chemical model of a plasma" for elements other than hydrogen.[44] The results obtained in this case are numerically close to those given by the ring approximation employed in the present paper.

Krasnikov[45] has calculated within the framework of the aforementioned expansion, supplementing the results of Ref. 42, the contribution of some of the terms of the next order ($\sim\xi^{5/2}$). Just as before, the relations obtained, when translated into the language of the "chemical model," have been proposed[46] for use for a plasma of elements other than hydrogen. The limited calculations performed in that reference for the case of argon and xenon show on the whole satisfactory agreement with the experimental results.[11,12] In view of the complexity of the final expressions obtained in Ref. 46, it is impossible in the present paper to compare directly the approximation proposed there with new experimental data and with results of calculations using the models (2–5) and (7–14). Partial comparison of the calculation of Ref. 46 indicates that these calculations are close to those obtained by using the "bounded atom" model used in the present paper.

[1]P. Caldirola and H. Knoepfel, eds. Physics of High Energy Density, Academic, 1971.
[2]S. I. Anisimov, A. Ya. Imas, G. S. Romanov, and Yu. V. Khodyko, Deistvie izlucheniya bol'shoĭ moshchnosti na metally (Action of High-Power Radiation on Metals), Nauka, 1970.
[3]V. M. Ievlev, Izv. Akad. Nauk SSSR, Énergetika i transport **6**, 24 (1977).
[4]G. É. Norman and A. N. Starostin, Teplofiz. Vys. Temp. **8**, 413 (1970).
[5]W. Ebeling, V. Kraft, and J. Cramp, Theory of Bound States and of Ionization Equilibrium in a Solid-State Plasma (Russ. transl.), Mir, 1979.
[6]S. G. Brush, H. L. Sahlin, and E. Teller, J. Chem. Phys. **45**, 2102 (1966).
[7]G. E. Norman, V. M. Zamalin, and V. S. Filinov, Metod Monte-Karlo v statisticheskoĭ termodinamike (The Monte Carlo Method in Statistical Thermodynamics), Nauka, 1977.
[8]B. N. Lomakin and V. E. Fortov, Zh. Eksp. Teor. Fiz. **63**, 92 (1972) [Sov. Phys. JETP **36**, 48 (1972)].
[9]A. V. Bushman, B. N. Lomakin, V. A. Sechenov, V. E. Fortov, O. E. Shchekotov, and I. I. Sharipdzhanov, Zh. Eksp. Teor. Fiz. **69**, 1624 (1975) [Sov. Phys. JETP **42**, 828 (1975)].
[10]R. H. Cristian and F. L. Yarger, J. Chem. Phys. **33**, 2042 (1955).
[11]V. E. Bespalov, V. K. Gryaznov, A. N. Dremin, and V. E. Fortov, Zh. Eksp. Teor. Fiz. **69**, 2059 (1975) [Sov. Phys. JETP **42**, 1046 (1975)].
[12]V. E. Fortov, A. A. Leont'ev, A. N. Dremin, and V. K. Gryaznov, Zh. Eksp. Teor. Fiz. **71**, 225 (1976) [Sov. Phys. JETP **44**, 116 (1976)].
[13]I. Ya. Dikhter and V. A. Zeĭgarnik, Dokl. Akad. Nauk SSSR **227**, 656 (1976) [Teplofiz. Vys. Temp. **13**, 483 (1975)].
[14]L. V. Al'tshuler, Usp. Fiz. Nauk **85**, 197 (1965) [Sov. Phys. Usp. **5**, 52 (1965)].
[15]V. E. Bespalov, V. K. Gryaznov, and V. E. Fortov, Zh. Eksp. Teor. Fiz. **76**, 140 (1979) [Sov. Phys. JETP **49**, 71 (1979)].
[16]A. A. Leont'ev and V. E. Fortov, Zh. Prikl. Mekh. Tekh. Fiz. No. 3, 162 (1974).
[17]Ya. B. Zel'dovich and Yu. P. Raĭzer, Fizika udarnykh voln i vysokotemperaturnykh gidrodinamicheskikh yavlenii (Physics of Shock Waves and of High-Temperature Hydrodynamic Phenomena), Nauka, 1966 [Academic, 1967].
[18]E. G. Popov and M. A. Tsikulin, Izluchatel'nye svoĭstva sil'nykh udarnykh voln v gazakh (Radiative Properties of Strong Shock Waves in Gases), Nauka, 1976.
[19]M. V. Zhernokletov, V. N. Zubarev, and G. S. Telegin, Zh. Prikl. Mekh. Tekh. Fiz. No. 4, 127 (1969).
[20]V. K. Gryaznov, I. L. Iosilevskii, and V. E. Fortov, Zh. Prikl. Mekh. Tekh. Fiz. No. 3, 70 (1973).
[21]L. D. Landau and E. M. Lifshits, Mekhanika sploshnykh sred (Fluid Mechanics), Gostekhizdat, 1954 [Pergamon].
[22]W. Ebeling, Physica (Utrecht) **38**, 378 (1968); **43**, 293 (1969).

[23]A. M. Semenov and E. E. Shpil'rain, in: Uravnenie sostoyaniya gazov i zhidkostei (Equation of State of Gases and Liquids), ed. by I. I. Novikova, Nauka, 1975, p. 77.
[24]D. A. Kirzhnits, Yu. E. Lozovik, and G. V. Shpatakovskaya, Usp. Fiz. Nauk **117**, 3 (1975) [Sov. Phys. Usp. **18**, 649 (1975)].
[25]J. M. Ziman, Calculation of Bloch Functions (Russ. transl.), Mir, 1977.
[26]J. O. Hirschfelder, C. F. Curtiss, and R. B. Bird, Molecular Theory of Gases and Liquids, Wiley, 1954.
[27]B. V. Zelener, Teplofiz. Vys. Temp. **15**, 893 (1977).
[28]E. A. Mason and T. H. Spurling, The Virial Equation of State, Pergamon, 1970.
[29]N. B. Vargaftik, Spravochnik po teplofizicheskim svoistvam gazov i zhidkostei (Handbook of Thermophysical Properties of Gases and Liquids), Nauka, 1972.
[30]G. M. Harris, J. Trulio, and J. Roberts, Phys. Rev. **119**, 1832 (1960).
[31]A. Sabukinas and A. Z. Chizhyunas, Lit. Fiz. Sb. **14**, 73 (1974).
[32]D. R. Hartree, Calculation of Atomic Structures (Russ. transl.), IIL, 1960.
[33]B. J. Alder and T. E. Wainraiht, J. Chem. Phys. **33**, 1439 (1960).
[34]H. C. Graboske, D. J. Harwood, and F. J. Rogers, Phys. Rev. **186**, 210 (1969).
[35]N. W. Ashcroft and J. Lekner, Phys. Rev. **145**, 83 (1966).
[36]W. G. Hoover, G. Stell, E. Goldmark, and G. D. Degani, J. Chem. Phys. **63**, 5434 (1975).
[37]B. V. Zelener, G. E. Norman, and V. S. Filinov, Teplofiz. Vys. Temp. No. 10, 1160 (1972).
[38]V. K. Gryaznov and I. L. Iosilevskiĭ, Chislennye metody mekhaniki sploshnoĭ sredy **4**, 166 (1973); in: Teplofizicheskie svoistva nizkotemperaturnoi plazmy (Thermophysical Properties of Low-Temperature Plasma), ed. by V. M. Ievleva, Nauka, 1976, p. 25.
[39]A. E. Glauberman and I. P. Yukhnovskiĭ, Zh. Eksp. Teor. Fiz. **22**, 562 (1952).
[40]F. H. Stillinger and R. Lowett, J. Chem. Phys. **49**, 1991 (1968).
[41]I. L. Iosilevskiĭ, Teplofiz. Vysok. temperature **18**, No. 2, 1980.
[42]A. A. Vedenov and A. I. Larkin, Zh. Eksp. Teor. Fiz. **36**, 1133 (1959) [Sov. Phys. JETP **9**, 806 (1959)]; A. I. Larkin, *ibid.* **38**, 1896 (1960) [**11**, 1363 (1960)].
[43]F. Rogers and H. De Witt, Phys. Rev. **8**, 1061 (1973).
[44]V. E. Fortov, B. N. Lomakin, and Yu. G. Krasnikov, Teplofiz. Vys. Temp. **9**, 869 (1971).
[45]Yu. G. Krasnikov, Zh. Eksp. Teor. Fiz. **73**, 516 (1977) [Sov. Phys. JETP **46**, 270 (1977)].
[46]Yu. G. Krasnikov and V. I. Kucherenko, Teplofiz. Vys. Temp. **16**, 43 (1978).

Translated by J. G. Adashko

The nonlinear theory of the current instability of short-wavelength drift oscillations

V. I. Sotnikov, V. D. Shapiro, and V. I. Shevchenko

Institute of Cosmic Research, Academy of Sciences of the USSR
(Submitted 23 July 1979)
Zh. Eksp. Teor. Fiz. **78**, 586–599 (February 1980)

We study the current instability of an inhomogeneous plasma, which leads to the excitation of short-wavelength drift oscillations with a frequency close to the lower-hybrid resonance. We show that the saturation of the instability is connected with the spectral transfer of the oscillations into the short-wavelength ragion, which is due to the modulational instability, and we determine the maximum amplitudes of the electrical fields of the oscillations. We evaluate the effective electron collision frequency due to the current instability and we show that the Parker-Sweet diffusion model for the reconnection of the magnetic field, modified to allow for the anomalous resistivity mechanism studied in the present paper, gives for the width of the magneto-pause an estimate that agrees satisfactorily with experiment.

PACS numbers: 52.35.Py

§1. INTRODUCTION

The instabilities of the currents flowing across a magnetic field are important both for laboratory plasmas (shock waves, theta pinch, turbulent heating) and for the plasma in the magnetosphere (magnetic field reconnection, anomalous resistivity in the boundary layers of the magnetosphere, and so on). One of these instabilities—the so-called "tearing" instability—is of an electromagnetic type.[1] It leads to the generation of a transverse magnetic field component both in thermonuclear magnetic bottles[2] and in the magnetosphere primarily in its tail part.[3]

At the same time, other kinds of instability are basically responsible for the occurrence of the anomalous resistivity; they lead to the excitation of potential or close to potential oscillations. The lowest threshold for excitation of them corresponds to the current instability for short-wavelength drift oscillations which are polarized in the plane at right angles to the magnetic field. Mikhailovskiĭ and Timofeev were the first[4] to study the linear theory of this instability and in Ref. 5 the fact that the oscillations may be non-potential, which in important for a plasma with a finite β (ratio of the gas-kinetic to the magnetic pressure), was taken into account.

 0038-5646/80/020295-08$02.40